Annual Report 1997

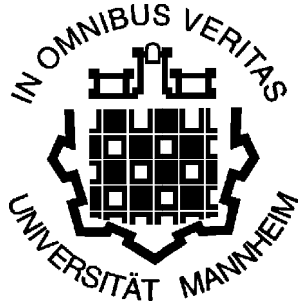

Chair of Optoelectronics
Faculty of Mathematics and Computer Science
University of Mannheim
B6,26
D - 68131 Mannheim
Telephone +49 (0)621 / 292 - 5459
Fax +49 (0)621 / 292 - 1605
EMail info@oe.ti.uni-mannheim.de

Inhaltsverzeichnis

1 Members of the chair of Optoelectronics

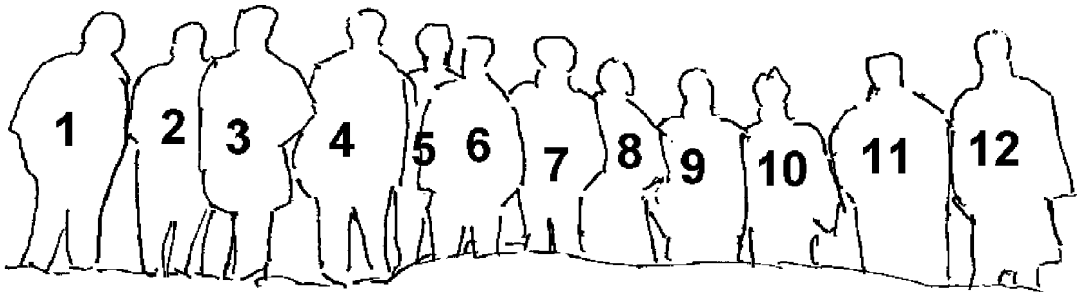

8	Dr. Bähr	Jochen	1615	jb@oe.ti.uni-mannheim.de
11	Prof. Dr. Brenner	Karl-Heinz	3004	brenner@rumms.uni-mannheim.de
2	Dietenhöfer	Eva	5459	dietenh@oe.ti.uni-mannheim.de
5	Fröning	Holger		maddock@rumms.uni-mannheim.de
3	Klug	Robert	1613	rklug@oe.ti.uni-mannheim.de
12	Dr. Krackhardt	Ulrich	5147	krackhdt@rumms.uni-mannheim.de
10	Kraf	Michael	1616	kraft@oe.ti.uni-mannheim.de
9	Million	Manuel Sebastian		manuelm@rumms.uni-mannheim.de
7	Oberhöffken	Arndt		wwwadmin@oe.ti.uni-mannheim.de
1	Passon	Christoph	5541	c.passon@oe.ti.uni-mannheim.de
6	Schiek	Steffen		schiek@rumms.uni-mannheim.de
4	Schmelcher	Thilo	5541	schmelch@oe.ti.uni-mannheim.de

2 Foreword

The chair of optoelectronics began its work in the summer of 1996 as one of the first chairs of the newly established course of studies, Technische Informatik (Computer engineering) at the university of Mannheim. Since this was one of the first technically oriented chairs in the faculty, special thank has to be attributed to the university adminstration for assisting in the fast formation of our experimental research environment. Several contributions in this report confirm, that after one year of constructing the labs, the component fabrication has now become routine. With three optics labs, one process laboratory and one clean room, the chair of optoelectronics is now in the position to continue its research in optical microintegration of components for optical communication and processing. Other research topics also have been included. So the facilities for measuring and testing, which were available in Erlangen, had to be reconstructed here. With one of my assistants, U. Krackhardt, also expertise in three-dimensional metrology was added.

The new students of computer engineering are now in their 3. Semester and it will take another two years until they begin their masters thesis (Diplom). Therefore we are very grateful that some of them are already helping in the labs on the basis of so called HIWI jobs.

This report describes the results of our efforts during this first year of research and we hope that the readers will find interest in some of these topics.

Karl-Heinz Brenner

3 Design tool for systems of stacked micro lenses

K.-H. Brenner

For the design of optical systems, ray tracing is commonly used. This approach is also valid for micro optical systems, since the effects of diffraction and refraction can be separated. If micro lenses fabricated by ion exchange in glass are to be included in the system analysis, ray tracing in inhomogeneous media is necessary. Conventional ray tracing software only supports a limited number of simple index models. Previous work has shown that the wave aberrations as well as the image quality depend very sensitively on the index distribution. We therefore have developed a design tool, which allows to take measured index distributions into account for computing the ray path. The simulation uses the standard Runge-Kutta algorithm to solve the differential equation

$$\frac{\partial^2 \vec{r}}{\partial \tau^2} = n\mathrm{grad}(n)$$

with the path element $d\tau = \frac{ds}{n}$. Presently implemented models of index distribution include cylindrical and spherical distributions with $n(r) = n_0 + \Delta n_{max} \cdot f(\frac{r}{r_0})$ and the normalized function $f(x)$ represented as a polynomial with order up to 12. The present model also includes spherical lenses and prisms with homogeneous index.

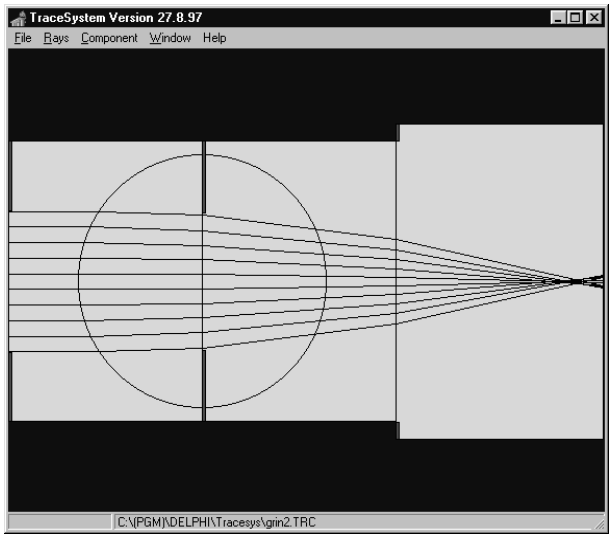

Fig. 1 Main window of design software

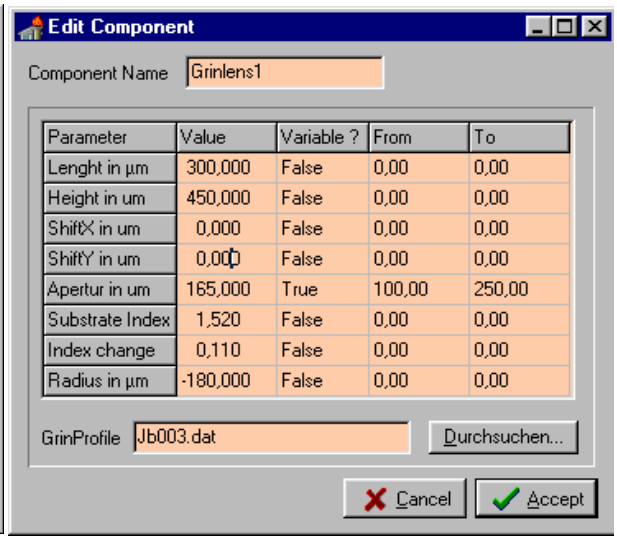

Fig. 2 Window for component editing

The parameters for describing a component are summarized in fig. 2 for the case of a GRIN lens. All the parameters of a component can be chosen as variable and modified interactively as shown in fig. 3. Thus the effects of modifying any parameter can be observed in real time since the trace update occurs in approx. 10 ms.

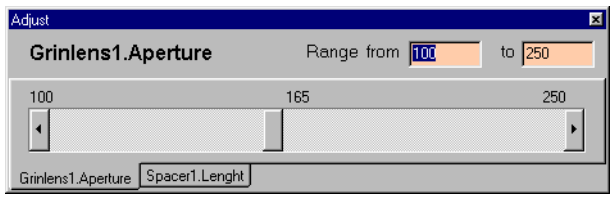

Fig. 3 Slider for interactive adjustment of variable system parameters

References

[2] J. Bähr, K.-H. Brenner, Realization and optimization of planar refracting microlenses by Ag-Na ion-exchange techniques, Applied Optics. 35, 5102-5107, (1996)

4 Demonstration of stacked microoptical system with large numerical aperture

R.Klug ,K.-H.Brenner

In the field of microoptics there is a demand for objectives with large numerical apertures (NA). An example is optical storage, where NA $>$ 0.5 is required. For planar micro lenses (PMLs) the NA is determined by the maximal index difference and the degree of exchange [2] and reaches typical values of 0.13-0.2. Thus stacking is needed to build high NA objectives from PMLs. As an example, we realized a confocal sensor head from four microlens arrays and from one pinhole array mask. The system design is shown in figure 1.

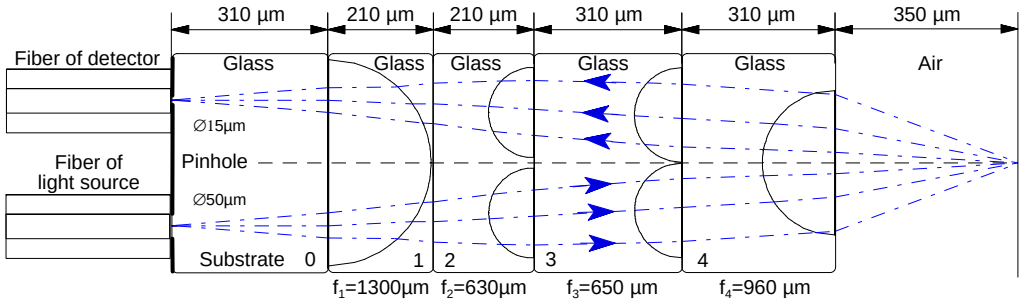

Figure 1: System design

The sensor is illuminated by a multimode fiber with a core diameter of 50 μm. The illuminating light travels through a 50 μm pinhole in substrate 0 and then through four microlens layers. The end of the illuminating fiber is imaged onto the optical axis of the fourth microlens with unit magnification. The working distance of the system is 350 μm. According to the confocal principle the light reflected or scattered from the object reaches the detector fiber only if the object is at the working distance. One important advantage of our design is that the illuminating light uses a different path than the reflected light, thus this system requires no beamsplitter and there are no disturbing backreflections in the system. We have realized an array of 16x32 confocal imaging systems on a grid with 500 μm x 250 μm pitch.

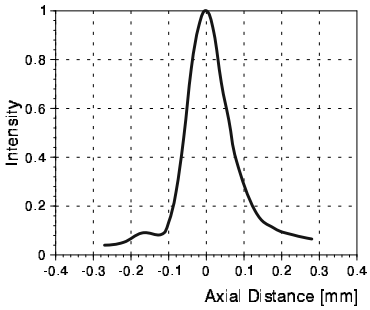

Figure 2: Axial response

The PMLs were fabricated by field assisted Ag-Na ion-exchange. The substrates were aligned under a microscope by the aid of concentric circles with 5 μm accuracy and fixed together with UV-curing glue. Figure 2 shows the axial response of the sensor head without pinholes, when a mirror at the output is scanned longitudinally. The full width at half maximum of the intensity is 100 μm, which is in agreement with the theory, if a pinhole of 50 μm diameter (fiber core) is assumed.

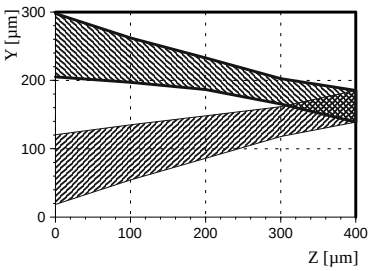

Figure 3: Light propagation after the sensor head

Figure 3 shows the measured light propagating in air behind the substrate 4 (S. Fig. 1), when detector fiber and source fiber are illuminated at the same time. The hatched area shows those locations, where the measured intensity exceeds the background noise. The slope of the outer lines in figure 4 is 0.328 rad, therefore the NA of the sensor head is 0.32. The entrance NA of the system on the fiber side is 0.17, while the NA of all PMLs is only 0.13.
We demonstrated, that optical system design can be applied to stacked microlenses and we have verified this design in an experiment.

References

[2] J. Bähr, K.-H. Brenner, Realization and optimization of planar microlenses by Ag-Na ion exchange techniques, Appl. Opt. 35, 5102-7 (1996)

5 Investigation of the stability of the algorithm for iterative index reconstruction

J. Bähr, K.-H. Brenner

The algorithm for reconstructing the 3D index distribution from interferometric measurements described in [1] was shown to be perfect for noiseless data and even for non monotonuous index distributions [4]. Here we report the stability of the algorithm for noisy data and measurement errors. For the simulation a random phase with a mean amplitude of 0.1λ was added to a given phase distribution, which is comparable to the accuracy of experimental data (fig. 1). The reconstruction then shows an increasing deviation in the center region (fig. 2). The statistic deviations were diminished by a subsequent low pass filtering of the reconstructed data. Fig. 3 demonstrates that the reconstruction then is in good agreement with the original index distribution. The reconstruction shows good stability against singular measurement errors, such as missing data. Although three sampling points were set to zero (fig. 4), the reconstruction shows good consistence with the original data in a sufficient distance from the measurement errors (fig. 5). Finally we investigated the sensitivity concerning the determination of the center of the phase distribution. If the sampling values are shifted laterally from the center of symmetry the geometry of the distribution is expected to be incorrect, which leads to wrong propagation lengths within certain zones of the distribution. For a radially symmetric distribution the lateral shift of the data can be expressed by the transformation $r_i' \to r_i + dx$ and $x_j' \to x_j + dx$. The light path in a single zone is given by

$$L(x_j', r_{j+1}') - L(x_j', r_j') = \sqrt{r_{i+1}^2 + 2r_{i+1} \cdot dx - x_j^2 - 2x_j \cdot dx} - \sqrt{r_i^2 + 2r_i \cdot dx - x_j^2 - 2x_j \cdot dx}$$

For examination of the outmost zone $j = i \quad \Rightarrow \quad x_j = r_j$ the light path can be written as

$$L(x_j', r_{j+1}') - L(x_j', r_j') = \sqrt{(r_i + \Delta x)^2 + 2(r_i + \Delta x) \cdot dx - r_i^2 - 2r_i \cdot dx} = \sqrt{2r_i \cdot \Delta x + \Delta x^2 + 2\Delta x \cdot dx}$$

with $r_{i+1} = r_i + \Delta x$ and Δx is the distance between the sampling points. According to the last equation the lateral shift becomes significant for the central zones for the calculation of the light path. Fig. 6 demonstrates the sensitivity to shifted data. In this example a shift of only two sampling points leads to an error of about 10% of the center value of the index distribution. From that point of view the central point of the phase distribution has to be determined very accurate.

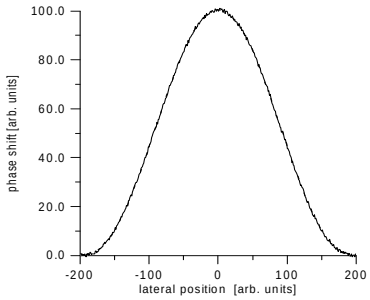

Fig. 1 noisy data of a phase shift

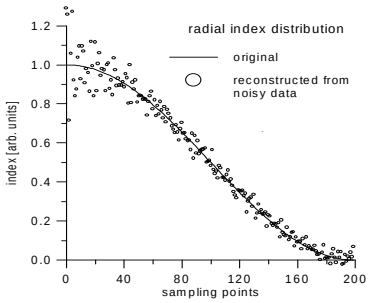

Fig. 2 reconstruction from noisy data

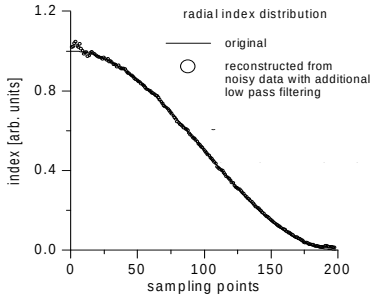

Fig. 3 reconstr. after low-pass filtering

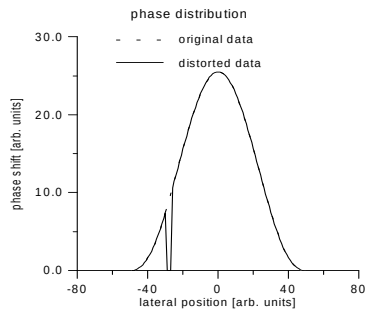

Fig. 4 defective phase data

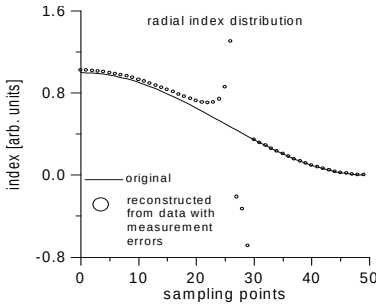

Fig. 5 reconstruction from defective data

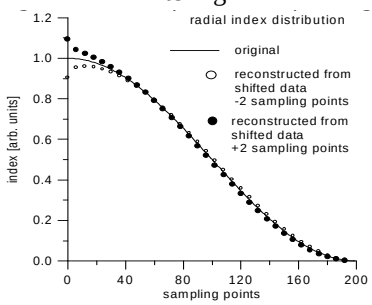

Fig. 6 incorrect reconstruction from shifted data

References

[1] J. Bähr, K.-H. Brenner, „Iterative reconstruction of a gradient index distribution from one interferometric measurement“, Optik,Int. J. for Light and Electron Optics 102, no. 3, 101-105 (1996)

[4] J. Bähr et al., „Concentric ring method“, annual report of the University of Erlangen (1993)

6 Comparison of several methods for measurement of the 3D index distribution

J. Bähr, K.-H. Brenner

In earlier works we demonstrated that the 3D index distribution can be reconstructed from only one interferometric measurement if the geometry of the distribution is known a priori [1]. In this article the results of the iterative reconstruction method (RA) are compared to those obtained by alternative methods such as the refracted near field method RNF [6], the diffraction tomography (DT) [10], data obtained by numerical simualtion and the investigation of thin slices [6]. The object under investigation was a two dimensional planar GRIN-lens, since the methods with exeption of the iterative algorithm and the diffractive tomography are resticted to 2-dimensional structures.
The measured phase distribution and the value of the width of the mask were the input data for the RA algorithm. For fabrication we used a line shaped mask aperture with a width of $80\mu m$ (fig. 1) in a thermal ion exchange process.
The RNF-measurement is reported to be accurate for measuring the index distribution of 2- dimensional index gradients like waveguides. The method is very sensitive to material absorptions. Therefore the method is limited to a depth of some tens of micrometers, which is sufficient for wave guides - but not for microlenses. For concentration profiles extending $150\mu m$ into the substrate the measurement is affected even by weak absorption, resulting in a measurement of higher index.
The DT method only responds to phase shifts and thus allows a measurement also for large depths. A problem associated with this method is the requirement of a continuous index distribution. This cannot be satisfied at the substrate surface since an index jump in the direction normal to the surface is inevitable. Due to this the index near to the substrate surface is measured inaccurate but for larger depths the method is very reliable.
The investigation of thin slices requires accurate knowledge of the thickness of the glass slice. The attainable resolution in this experiment is therefore limited at 10^{-2}. The numerical simulation of the ion exchange process in fig. 2 was done with the k-parameter model [7] for a k value of 3. In the region under the surface the RA shows good agreement with the RNF data and the results of the thin slice investigation. For larger depth the data fit very well to those of the DT.

To summarize the RA can be used for a characterisation of the threedimensional index distribution. It shows good agreement to the DT and RNF where thode methods are applicable.
The autors thank W. Singer, B. Dobler and B. Messerschmidt for the DT, the RNF and the thin slice measurement.

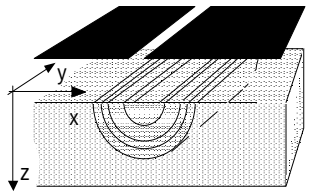

Fig. 1 2-dimensional planar microlens by thermal ion exchange process

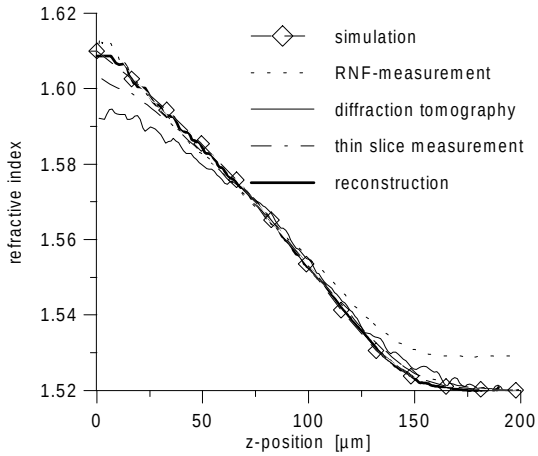

Fig. 2 Comparison of the the refracted index profile reconstructed by several methods

References

[1] J. Bähr, K.-H. Brenner, terative reconstruction of a gradient index distribution from one interferometric measurement“, Optik, Int. J. for Light and Electron Optics 102, no. 3, 101-105 (1996)
[6] R. Göring, M. Rothardt, „Application of the refracted near-field thenique to multimode planar channes waveguides in glass“, J. Opt. Commun. 7, 82-85 (1986)
[7] K. Iga, M. Oikawa, S. Misawa, J. Banno, Y. Kokubun, „Stacked planar optics: an application of the planar microlens“, Appl. Opt. 21, 3456-3460 (1982)
[10] W. Singer, B. Dobler, H. Schreiber, K.-H. Brenner, „Refractive index measurement of gradient-index microlens by diffraction tomtography“, Appl. Opt. 35, 2167-2171 (1996)

7 Rastered Grey–Tone Masks written by Laser–Lithography

K.-H. Brenner, U.W. Krackhardt

The most common application of laser lithography (see also article in this report) is binary structuring of a substrate. However, there are some applications requiring quasi–analog transmission either with respect to phase or amplitude. That is, phase gratings or grey–tone masks with multilevel or even continuous distributions have to be realized [5].
A well known technique for fabricating continuous phase structures is to spatially control the exposure dose. This, however requires special and expensive extra equipment of the lithographic machine.
Provided the lithographic process can handle smaller structures than can be resolved by the optical system in which the fabricated component will be used, a binary coding of continous levels is sufficient. In this approach, we applied a technique for rastering grey level images, which was developed by us earlier. The technique choosen, is based on clustered threshold matrices since it provides very good greytone linearity and good seperation of the spatial object spectrum and the carrier spectrum.
The substrate constists of a glass substrate, a chromium film and a photoresist layer on top.

First the photo restist layer is structured by lithographic exposure and subsequent developing. Then, the regions not covered by photoresist are accessible by a wet–chemical process step, which removes the chromium film. Thus, an amplitude mask is obtained.
Taking into account the limitations of our lithographic process (see an other article in this report), we managed to compose any raster pattern (see fig. 2) by elementary features (squares) with minimum edge size of $1.6\mu m$. Figure 1 shows a section of a rastered sinusoidal intensity profile. The smallest features are squares of $2\mu m \times 2\mu m$. The component was fabricated for use in optical 3D–metrology with fringe projection technique [3].

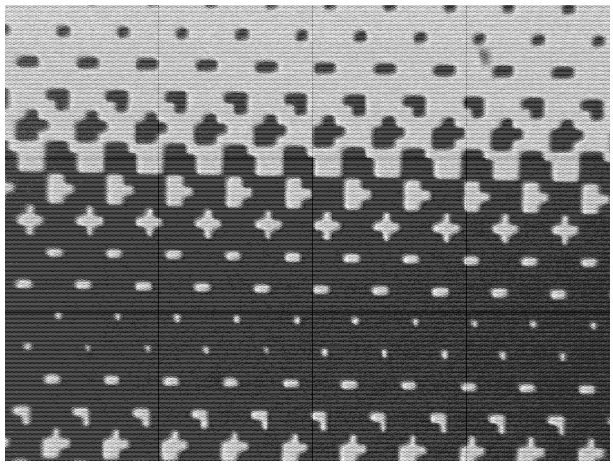

Fig. 1: Micrograph of a $160\mu m$-wide section of a rastered sinusoidal intensity profile

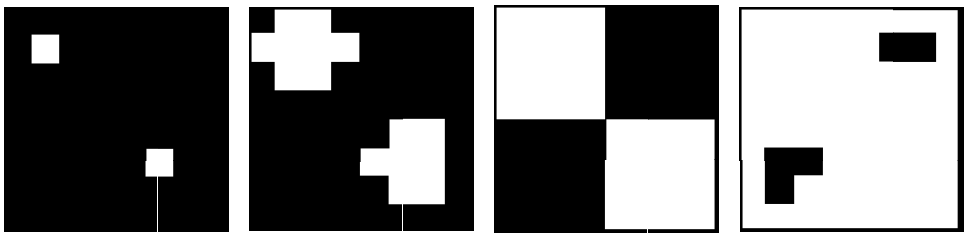

Fig. 2: Sub–set of raster patterns of a dither–cell consisting of 8x8 elementary features.

References

[3] B. Breuckmann, "Bildverarbeitung und optische Meßtechnik in der industriellen Praxis", Franzis' Verlag, ISBN 3-7723-4861-0, 124 - 154 (1993)
[5] M. T. Gale, "Micro-Optik", H.-P. Herzig, ed., ISBN 0-7484-0481-3, 87-126 (1997) Optik, Int. J. for Light and Electron Optics 102, **3**, 101-105, (1996)

8 Laboratory Facilities

U.W. Krackhardt, M. Kraft

The chair of Optoelectronics has installed laboratories for chemical and lithographic processing and for optical research.
The lithographic processing is performed in a **cleanroom**:
Subtrates (e.g. glass, fused silica, or Si) coated with photoresist are structured by means of a **laser lithrography machine** DWL 2.0 from Heidelberg Instruments.

A laser beam (HeCd, 442 nm) is focussed on the substrate surface. The substrate is placed on a moving table which is position controlled by an interferometer. The machine is capable of writing structures with a minimum feature size of 0.8 μm within an address raster of 50 nm. Since the DWL is a matrix writer, the writing time is independent of the complexity of the structure but depends on the overall area to be exposed. An area of about 3 cm x 3 cm can be written within 40 min., approximately. For multilayer exposures the machine is equipped with an alignment facility providing an accuracy of 200 nm.

Landscape of the clean room

For multi–layer lithography the substrate has to be recoated with photoresist between each subsequent lithographic exposure. This is done with a **photoresist spinner** which offers high reproducability due to programmable spinning profiles and automatic control of photoresist dose.
A subseqent exposure can be performed either pointwise by laser lithography or in one step by a **mask aligner** with a lateral accuracy of $\pm 0.5 \mu m$.

A **Reactive Ion Etching** (RIE) machine is available to transfer the structure from the photoresist layer into glass (e.g. for computer holography). Based on a physical/chemical process glass (fused silica) is removed at regions not coated by photoresist.
For characterization purpose a **microscope** (max. magnification 1200:1) equipped with a CCD-camera and a PC-based frame grabber is used for computer aided process control. Especially for characterization of surface profiles a PC controlled tactile **profiler** with a depth resolution of down to 50 nm is applied.

Our three **optic laboratories** are each equipped with a vibration damped table that serves as a work bench for optical hardware development.
One of these laboratories is used for optical metrology. For the measurements of optical path lengths **interferometers** of the Mach–Zehnder– and the Linnik–type can be used. The software is described in an other article of this report.

In a **process laboratory** an electron sputter machine enables the deposition of metallic layers onto substrates. This is useful e.g. for for realization of opto–electronic circuit boards or for the in-house fabrication of substrates which are used for ion–exchange in glass (see an other article in this report). The set–up for ion–exchange is also placed in this process laboratory.

9 Transmission Interferometer for Phase Elements (Mach-Zehnder-Type)

Christoph Passon

To measure the phase profile of optical elements in the submillimeter range an interferometer has been set up. The setup presents a typical Mach-Zender interferometer with the reference and the measurement path forming a rectangle (see fig.1). At the input beamsplitter (5) two different light sources can be feed into the system . At the output beamsplitter (10) the two optical paths are joined and interfere in the image plane (12).

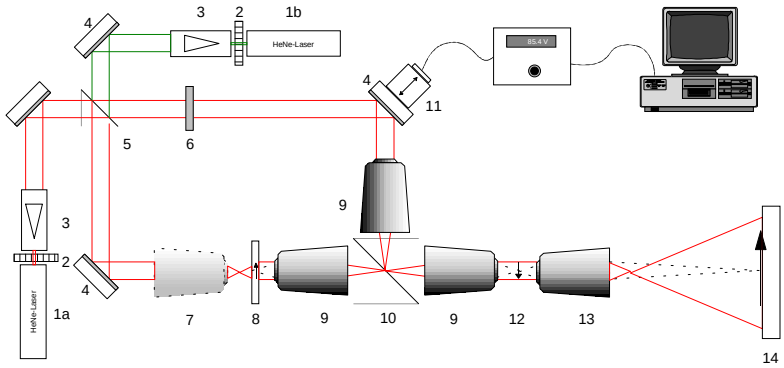

Fig 1: Mach-Zehnder Interferometer Setup

In the reference path the deflecting mirror (4) at the corner of the optical path is mounted on a piezo actuator (11), which can be controlled by a computer. The piezo actuator is supplied with a capacitive distance meter supporting position control in the sub nanometer range.

A revolver with a selection of 4 grey filters in the reference path offer the ability to adjust differences of brightness between light from the reference and the measurement path, which result from absorbtions of the test object (8). Identical microscope objectives (9) at the end of the reference and measurement paths image the object plane to the image plane with zero phase difference when no object is inserted in the measurement path. An optional microscope objective (7) in front of the test object can be inserted in the measurement path to test spherical phase elements by illuminating the test object with a sperical wave and measuring the difference between the resulting plane wave from the test element and the plane wave from the reference path. A selection of microscope objectives (13) mounted on a revolver in the exit path of the interferometer produce images at different magnification on the CCD camera (1 x, 2.5x, 5x). With these magnifications the fieldsize on the CCD is 300 μm, 600 μm, 1.5 mm respectively.
The complete setup is mounted on a bread board with 90 cm x 60 cm and is shielded against air turbolences by a plastic case of 50 cm height. The system is controlled by a standard PC equipped with a frame grabber board. The piezo actuator is driven with a control box which is connected to the PC via a serial port. The test object holder is mounted on a xyz stage, providing abilaty to measure a field of 10 cm x 10 cm size. The manual controls of the xyz stage are planned to be exchanged with computer controlable actuators to allow fully automized measurement of the full measurement field.

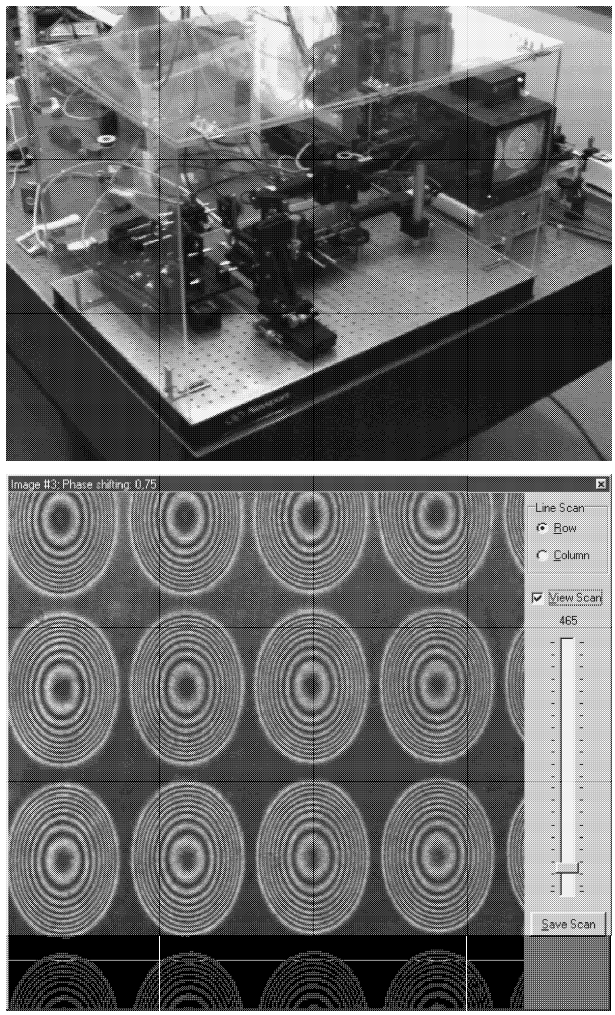

Interferogramm of a μ-lens-array (pitch 250 μm)

10 PSM — Software for Phase Shift Interferometry

K.-H. Brenner, U.W. Krackhardt, S.M. Million, C. Passon

In order to optically characterize components like micro lenses made by ion exchange [1] or computer holograms [8] PC controlled interferometers (Mach–Zehnder– and Linnik–Type) have been set up. The software for controlling the interferometers and for evaluating fringe data has been written in–house, since this allows for quick and easy implementation of the latest algorithms for measurement, evaluation and presentation.
Gernerally, the software can do metrology with any kind of fringe data obtained by real or synthetic phase shifting. Therefore the software is called **PSM** as an acronym for Phase Shift Metrology. PSM has been written in PASCAL with a tool for Rapid-Application Development (RAD) under MS-Windows 95.
The essential goals for the design of this software are:

1. Intuitive user interface
2. Ease of functionality upgrade, i.e adding new operations
3. Universality with respect to the type of the phase shift interferometer
4. Flexibility with respect to hardware (frame grabber, phase shift controller)
5. Off-line functionality, i.e. data evaluation without interferometer hardware attached to the PC, should be supported

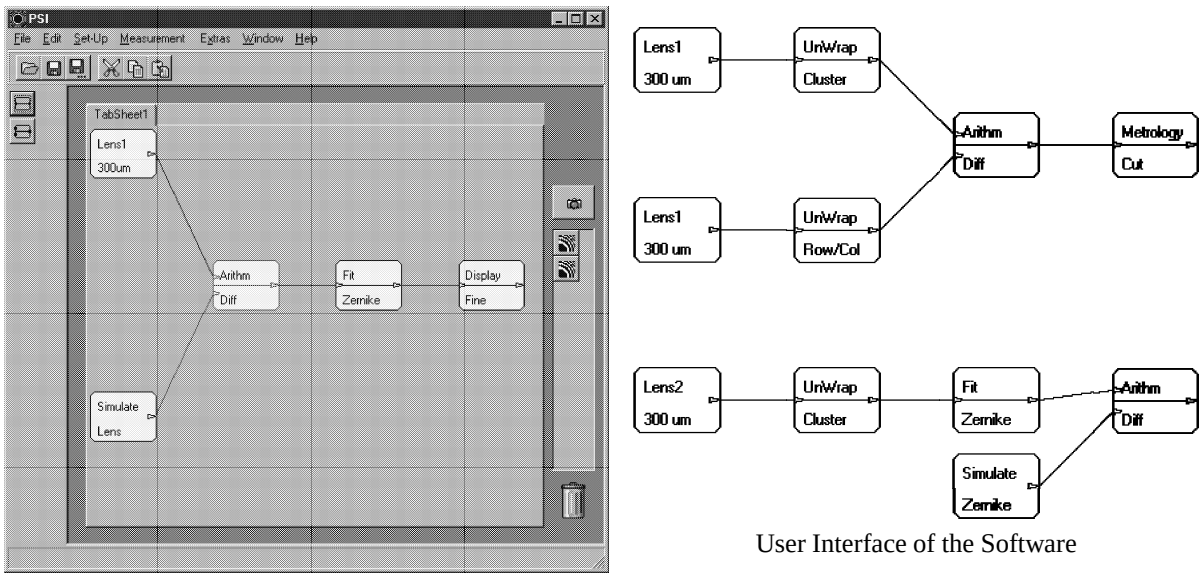

User Interface of the Software

The user interface has to support the handling of a huge amount of operations known in fringe analysis. We realized a both flexible and intuitive software interface (GUI) that represents the data flow graphically by operators and links.
An operator can be selected from a dialog similar to the file selector box, whereby the directories provide a classification scheme for the set of operators. The operators are displayed similar to files with attributes like name of the operator, I/O specifications, comments, creation time, etc. An operator is inserted into the flow chart by a simple drag–and–drop action. For ease of upgrading functionality the operators are collected in DLL–files that can be dynamically linked to the main programm. For a further increase of convenience each user can set up his individual GUI profile.

References

[1] J. Bähr, K.-H. Brenner, "Iterative reconstruction of a gradient index distribution from one interferometric measurement", Optik, Int. J. for Light and Electron Optics 102, **3**, 101-105, (1996)
[8] U. Krackhardt, N. Streibl, J. Schwider, "Fabrication errors of computer generated multilevel phase-holograms", Optik 95, **4**, 137 - 146 (1994).

11 Fabrication of integrated GRIN-ROD lenses

J. Bähr, K.-H. Brenner

The typical way to fabricate GRIN-ROD lenses is the preparation of single glass cylinders in a ion exchange process [9]. For integrated optic applications an additional alignment step is neccessary. In this artice we report a fabrication method for integrated GRIN-ROD lenses.
As reported earlier GRIN-elements with nearly ideal radial symmetry are obtained using spot like mask apertures in a field assisted ion exchange process [2]. With transition to line shaped masks with a width of a few microns, cylindrical distributions can be realized. According to fig.1 two substrates with semi-cylindrical distribution can be assembled to attain integrated full-cylinder-ROD lenses. Since the mask is structured in a photolithographic process the lateral accuracy of the position of the elements is the same as that at the photolithographic process. In addition, for further machining alignment marks can also be realised on the substrate simultaneously in the same structuring process.

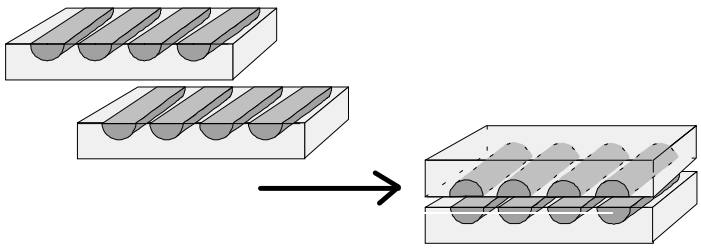

Fig. 1 assembling of two half-cylinder ROD arrays

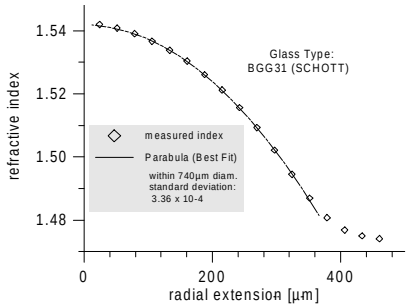

Fig. 2 radial index distribution

With the field assisted ion exchange process nearly steplike index distributions are obtained. For imaging application a radial index distribuiton with the shape of

$$n(r) = n_0 \mathrm{sech}(\sqrt{A}\cdot r) \cong n_0\left(1-\frac{Ar^2}{2}\right);\quad n(z) = const \quad \text{where} \quad A = \frac{2\cdot\Delta n_{max}}{(n_0+\Delta n_{max})\cdot r_{ROD}^2}; r \le r_{ROD}$$

is required. In this notation n_0 is the refractive index of the glass substrate. To achieve this distribution a post heating process is employed (fig. 2). Since this is an isotropic process the symmetry of the element is conserved [2]. With the applied silver-sodium ion exchange process we attain an index increment Δn of 0.11 in our substrate glasses. According to equation

$$NA_{max} = \sqrt{\frac{2\cdot\Delta n_{max}}{n_0 + 3\cdot\Delta n_{max}}}$$

we achieve a numerical aperture of 0.35 (fig.3). For verification a test pattern was imaged by a half-pitch GRIN-ROD. Fig. 4 demonstrates the good resolution of the GRIN-ROD, that is comparable to the resolution of microscope objective with a numerical aperture of 0.35 (fig. 5).

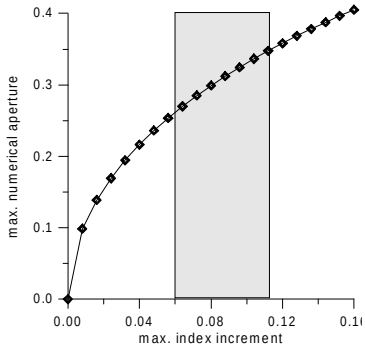

Fig. 3 achievabel numerical apertures

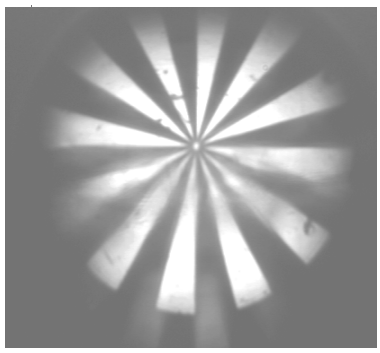

Fig. 4 image of a test pattern with the ROD-lens

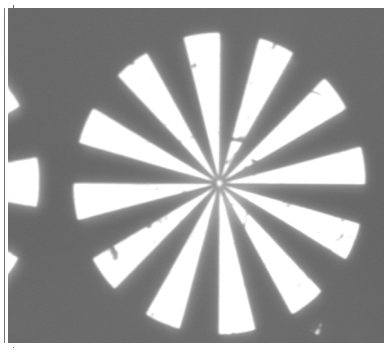

Fig. 5 image with an microskope objective (N.A.=0.35)

References

[2] J. Bähr, K.-H. Brenner, „Realization and optimization of planar refaktive microlenses by Ag-Na ion exchange techniques“ Appl. Opt. 35, 5102-5107 (1996)
[9] B. Messerschmidt, T. Posner, R. Göring, „Colorless gradient-index cylindrical lenses with high numerical apertures produced by silver-ion exchange“, Appl. Opt. 34, 7825-7830 (1995)

12 Mask-optimization for fabrication of microlens arrays with a high fill-factor

J. Bähr, K.-H. Brenner

For parallel data processing with microlens arrays a high lateral fill-factor is required to utilize the substrate area. In our institute microlens arrays are fabricated by field assisted ion exchange processes with diffraction limited performance and numerical aperture upto 0.2 [2]. To get a high lateral fill-factor the mutual influence of ion currents through adjacent mask windows has to be considered, because this effects a deviation from the symmetry of the microlens (fig. 1) that results in non symmetric on-axis aberrations. It has been shown, that symmetric lens aberrations can be supressed efficiently by an additional post heating step [2, 11]. Thus it is important to avoid non symmetric on-axis aberrations already in the field assisted process step.
We investigated the deviation from the cylindrical symmetry in an array with cartesian arrangement by calculation of the wavefront aberrations from simulated data. The pitch has a value of $250\mu m$. Fig. 2 shows the standard deviation from the wavefront $\sigma(w)$ versus the lateral radius of the microlens. For diffraction limited performance $\sigma(w)$ has to be less than $\lambda/14$. For circular mask apertures the aberrations get significant with increassing lateral extension. Using extended mask apertures these aberrations could be reduced by screen-off effects. But in this case the optical power would be decreased, because the extension of those lenses in the volume is reduced [2]. To achieve an aspect ratio of 1 between lateral and transversal extension with respect to the $\lambda/14$-criterion we found a maximum lateral diameter of 65% of the pitch using a mask with an aperture of $40\mu m$.
This value could be increased by optimization of the geometry of the mask. Fig. 3 shows the shape of the mask and the topography of the simulated microlens. For a small lateral extension the lens shape shows a strong deviation from cylindrical symmetry (fig. 4), because of the asymmetric shape of the mask. With increasing extension this deviation is compensated by the mutual influence of ion currents. At a certain point we obtain a minimum (fig. 4). Using a mask with an edge width of $70\mu m$ we obtained a maximum lateral diameter of 85% of the pitch. Futher increase of the lateral extension again diminishes the radial symmetry of the microlens.

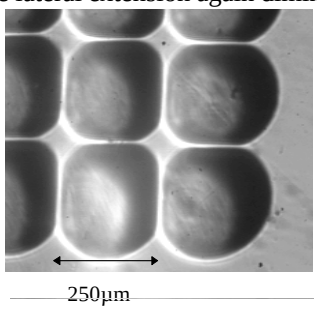

Fig. 1 distorsion of symmetry in a cartesian array

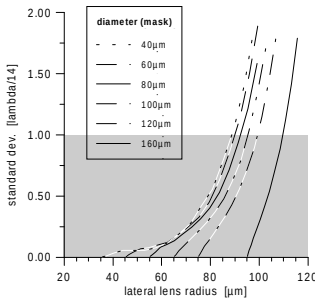

Fig.2 $\sigma(w)$ for different circular mask apertures

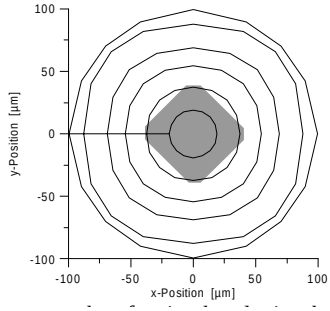

Fig. 3 topography of a simulated microlens using a optimized mask aperture

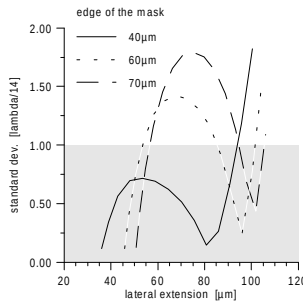

Fig. 4 $\sigma(w)$ for different optimized mask apertures

References

[2] J. Bähr, K.-H. Brenner, „Realization and optimization of planar refaktive microlenses by Ag-Na ion exchange techniques“ Appl. Opt. 35, 5102-5107 (1996)
[11] W. Singer, M. Testorf, K.-H. Brenner, „Gradient-index microlenses: numerical investigation of different spherical index profiles with the wave propagation method“, Appl. Opt. 34, 2165-2171 (1995)

13 Parallel optical fiber plug

Christoph Passon

The concept of parallel optical connectors using beam collimation coupling was developed for an optical backplane in a 19” computer rack. Using this coupling principle for parallel optical connections demands very high precision during manufacturing. To simplify the assembly of the parts, V-grooves are used to hold the fibers. This reduces the numbers of degrees of freedom in the positioning of the fibers with respect to the lenses. In the experimental realization the V-grooves were fabricated by injection molding, using Si-grooves as master by University of Dortmund. The front surfaces also possess an angle of 54^o and serve as mirrors for deflecting the light out of the substrate. This angle has the advantage that back reflections are reduced considerably compared to a 45^o angle. For angled fiber front faces the total isolation from back reflections reaches a value of approx. 150 dB. The mirrors are coated with silver and have a reflectivity of 98 %.

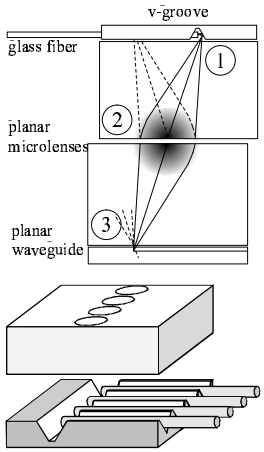

Fig. 1 Scheme of the parallel optical connector

A planar microlens array is used to collimate the beams. This array has to be positions with respect to the V-grooves so that for each channel, after reflection, the optical axis of a fiber meets the center of the corresponding lens. The required accuracy here is approx. $0.5 \mu m$.

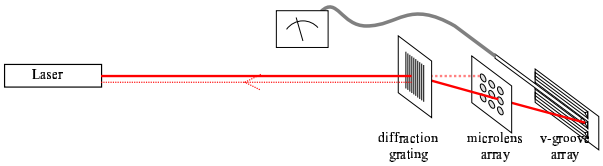

Fig. 2 Alignment setup using a diffraction grating as angle reference

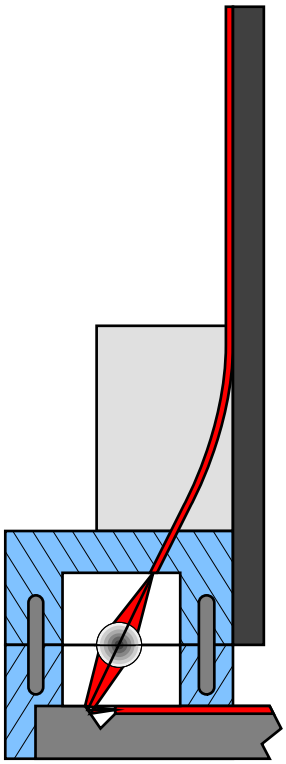

For positioning the micro lenses, three degrees of freedom have to be adjusted: the x-y-direction and the angular φ around the rotation axis. For adjusting the x-y-position, the collimated beam behind the lens would have be set to 54^o, which is difficult to verify. Therefore we have fabricated a reference grating (fig. 2) , which is placed between the laser and the micro lens array and the optimum position is determined by maximizing the optical power coupled into the fiber. The thickness of the lens substrate is adapted to the focal length of the microlenses. The lens coupling system was also used to connect to planar waveguides. The scheme for a fiber-waveguide connector is shown at the left side. For the back plane isotropic and anisotropic etching processes are used to produce the waveguides and the mirror. Taking all possible sources of loss in the connector into account, the different contributions are due to

- optical System -0.40 dB
- mirror -0.09 dB
- misalignment -0.10 dB
- absorption in the filling polymer -0.05 dB

and the total coupling efficiency should assume a value of 0.64 dB.

A List of Publications

Literatur

[1] J. Bähr and K.-H. Brenner. Iterative reconstruction of a gradient index distribution from one interferometric measurement. *Optik, Int. J. for Light and Electron Optics 102*, (3):101–105, 1996.

[2] J. Bähr and K.-H. Brenner. Realization and optimization of planar refracting microlenses by ag-na ion-exchange techniques. *Applied Optics*, 35:5102–5107, 1996.

[3] B. Breuckmann. pages 124 –154. Franzis' Verlag, 1993. ISBN 3-7723-4861-0.

[4] J. Bähr et al. Concentric ring method. Annual report, University of Erlangen, 1993.

[5] M. T. Gale. pages 87–126. Taylor & Francis, 1997. ISBN 0-7484-0481-3.

[6] R. Göring and M. Rothardt. Application of the refracted near-field technique to multimode planar channes waveguides in glass. *J. Opt. Commun.*, 7:82–85, 1986.

[7] K. Iga, M. Oikawa, S. Misawa, J. Banno, and Y. Kokubun. Stacked planar optics: an application of the planar microlens. *Appl. Opt.*, 21:3456–3460, 1982.

[8] U. Krackhardt, N. Streibl, and J. Schwider. Fabrication errors of computer generated multilevel phase-holograms. *Optik 95*, 4, 1994.

[9] B. Messerschmidt, T. Posner, and R. Göring. *Appl. Opt.*, 34:7825–7830, 1995.

[10] W. Singer, B. Dobler, H. Schreiber, and K.-H. Brenner. Refractive index measurement of gradient-index microlens by diffraction tomtography. *Appl. Opt.*, 35:2167–2171, 1996.

[11] W. Singer, M. Testorf, and K.-H. Brenner. Gradient-index microlenses: numerical investigation of different spherical index profiles with the wave propagation method. *Appl. Opt.*, 34:2165–2171, 1995.